Adaptive Trellis-Coded Modulation over Predicted Flat Fading Channels

Sorour Falahati*, Arne Svensson†, Mikael Sternad* and Hong Mei‡

*Department of Signals and Systems, Uppsala University, P.O. Box 528, SE-751 20 Uppsala, Sweden.
Email: {Sorour.Falahati, Mikael.Sternad}@signal.uu.se
†Department of Signals and Systems, Chalmers University of Technology, SE-412 96 Göteborg, Sweden.
Email: Arne.Svensson@s2.chalmers.se
‡Department of Information Technology, Uppsala University, P.O. Box 337, SE-751 05 Uppsala, Sweden.
Email: Mei.Hong@it.uu.se

***Abstract*— We consider the optimum design of an adaptive scheme based on TCM and predicted CSI for flat Rayleigh fading channels, intended for fast link adaptation. The question of how to optimally adjust the data rate to maximize the spectral efficiency, subject to a BER constraint when imperfect CSI is taken into account, is answered. An optimum solution based on the predicted SNR and the prediction error variance is derived. The performance of the adaptive TCM scheme is illustrated by utilizing seven 4-D trellis codes based on the International Telecommunications Union's ITU-T V.34 modem standard. The results indicate that the gain in spectral efficiency by adaptive TCM is about 1-2 dB compared to adaptive uncoded M-QAM, for most of average SNRs. Finally, the performance of the adaptive TCM and in particular, its loss at high SNRs compared to adaptive uncoded M-QAM, are investigated in details.**

I. Introduction

The problems of spectrum utilization in the mobile environment stimulate a great deal of research, especially in the area of adaptive transmission. The purpose of adaptive transmission is to adjust the signaling parameters as the channel varies, with the best possible usage of resources. Recently, adaptive transmission based on uncoded M-ary Quadrature Amplitude Modulation (M-QAM) has gained considerable attention [1]–[4]. To improve the obtainable spectral efficiency, more complex schemes would be required. A competitive candidate for this purpose is Trellis-Coded Modulation (TCM) [5]–[8]. The reason is that a TCM scheme has the potential of attaining a target Bit Error Rate (BER) at a lower average Signal-to-Noise Ratio (SNR), as compared to an uncoded M-QAM with the same spectral efficiency.

The adaptive transmission techniques often rely on the Channel State Information (CSI) being available at the transmitter. Perfect CSI is usually assumed in the design of adaptive modulation schemes. However, in order for the scheme to meet the expectations in practice, realistic assumptions should be used in the design [1], [2], [4], [8], [9]. An important requirement is that the CSI often needs to be available a few slots ahead to setup the transmission. For very slowly fading channels, the outdated estimates of CSI are still useful for the adaptation purposes. However, for fast fading channels, the feedback delays result in inaccurate CSI estimates at the time of transmission. Hence, it is logical to perform fast link adaptation based on channel predictions.

The optimum adaptive TCM scheme considered here, adjusts the data rate such that the spectral efficiency is maximized subject to a target BER and constant average transmit power. The scheme takes the statistical information of predicted Rayleigh fading channels into account. This approach distinguishes the present work from other solutions found in the literature (see e.g. [5]–[7]). The channel predictions utilized in this study are obtained through an unbiased quadratic regression of the past noisy channel estimates [10]. The statistical information is exploited to improve the overall system performance and to fulfill the BER requirements even in presence of the prediction error.

The spectral efficiency of the adaptive TCM is evaluated and compared with the adaptive uncoded M-QAM. The results show that the expected gain in spectral efficiency based on TCM is obtained for a large but limited range of average SNR. At high SNRs, superior performance by the uncoded M-QAM is observed. Detailed investigations show that this phenomenon is caused by the impact of the prediction quality on the rate boundaries as well as the higher rate transmission of uncoded M-QAM.

In the following, Section II describes the system model, the structure of the TCM scheme and the statistical characteristics of the channel predictor. The optimal rate adaptation is derived in Section III under a BER constraint. Analytical results are presented in Section IV and are discussed in detail. Finally, Section V summarizes the results.

II. System model

TCM schemes with different constellation sizes are provided at the transmitter. The channel is modeled by a flat Rayleigh fading channel with AWGN. At the receiver, a channel estimator estimates the channel gain which is used to perform coherent detection of the data bits. A time-series of these channel estimates are used for prediction purposes. Based on

Hong Mei contributed in this work during her studies at Chalmers University of Technology in Göteborg, Sweden.

This work was funded by the *Swedish Foundation for Strategic Research*.

the predicted channel and the prediction quality, a constellation size is selected and reported to the transmitter via the feed-back channel. There, the adaptive trellis encoder maps the incoming data bits to the symbols belonging to the selected constellation where constant average power is assumed.

Let r_n denote the received signal sampled at time nT_s where T_s is the symbol period and index n represents the signal sample at the symbol rate. Here, r_n is given by

$$r_n = s_n g_n + w_n, \tag{1}$$

where s_n is the transmitted symbol with average transmit power $\bar{S}$. Moreover, w_n is a sample of a complex AWGN with zero mean and time-invariant variance σ_w^2. Finally, g_n is the complex channel gain with circular Gaussian distribution with zero mean and a variance denoted by σ_g^2. The channel gain power denoted by $p_n = |g_n|^2$, which is proportional to the instantaneous received SNR, is then $\chi^2(2)$ distributed. The auto-correlation function of the channel gain is determined by the Doppler spectrum. The average received SNR is given by $\bar{\gamma} = \bar{S}\sigma_g^2/\sigma_w^2$. For the constant transmit power assumed here, the instantaneous received SNR is $\gamma_n = \bar{\gamma} p_n/\sigma_g^2$ and the predicted instantaneous received SNR is $\hat{\gamma}_n = \bar{\gamma}\hat{p}_n/\sigma_g^2$ where $\hat{p}_n$ is the predicted instantaneous channel gain power.

Since the channel estimation error is believed to have a minor effect on the performance compared to the prediction error, perfect channel estimation is considered here for the demodulation. Also, to perform decoding at the rate used by the encoder at any time instant, an error free feed-back channel is assumed. Moreover, the prediction horizon is presumed to be long enough to take the computational and signaling delays in the adaptation control loop into account.

The proposed adaptive TCM scheme utilizes a set of L two-dimensional ($2L$-D) trellis-codes with different constellation sizes, similar to [7], where L is a positive integer. Let N denote the number of constellations available at the transmitter, each of size M_i with $k_i = \log_2 M_i$ bits per symbol for $i = 1, \cdots, N$. A $2L$-D signal constellation is obtained by L-fold Cartesian products of 2-D signal constellations. At every Lth transmission time instant, $K = L \times k_n$ coded bits are mapped onto L symbols, each from a 2-D constellation of size M_i for $i = 1, \cdots, N$. These symbols are sent during L consecutive symbol intervals. At the receiver, soft decoding based on the Viterbi algorithm is performed where the squared Euclidean distance is used as metric in the decoder.

The channel gain is predicted using an unbiased quadratic power predictor proposed in [10] which is optimal in the Mean Square Error (MSE) sense. For this type of predictor, the error variance of the predicted channel gain, denoted by $\sigma_{\epsilon_c}^2$, is related to the error variance of the predicted power, denoted by $\sigma_{\epsilon_p}^2$, as [11]

$$\sigma_{\epsilon_p}^2 = \sigma_{\epsilon_c}^2(2\sigma_g^2 - \sigma_{\epsilon_c}^2). \tag{2}$$

In this work, $\sigma_{\epsilon_p}^2$ is used as a measure indicating the *prediction quality*, where the higher it is, the less reliable the predicted values become. In section 8 of [11], it is shown that if an optimal unbiased power predictor is used which provides a given $\sigma_{\epsilon_c}^2/\sigma_g^2$, then the pdf of the instantaneous true SNR γ_n, conditioned on the instantaneous predicted SNR $\hat{\gamma}_n$, will be

$$f_\gamma(\gamma|\hat{\gamma}) = \frac{\mathrm{U}(\gamma)\mathrm{U}(\hat{\gamma} - \bar{\gamma}\sigma_{\epsilon_c}^2/\sigma_g^2)}{\bar{\gamma}\sigma_{\epsilon_c}^2/\sigma_g^2} \exp\left[-\frac{\gamma + \hat{\gamma} - \bar{\gamma}\sigma_{\epsilon_c}^2/\sigma_g^2}{\bar{\gamma}\sigma_{\epsilon_c}^2/\sigma_g^2}\right] \mathrm{I}_0\left(\frac{2}{\bar{\gamma}\sigma_{\epsilon_c}^2/\sigma_g^2}\sqrt{\gamma(\hat{\gamma} - \bar{\gamma}\sigma_{\epsilon_c}^2/\sigma_g^2)}\right), \tag{3}$$

where $\mathrm{U}(\ )$ is the Heaviside's step function and $\mathrm{I}_0(\ )$ is the zeroth order modified Bessel function. The time index n was dropped in the pdf expression since γ_n and $\hat{\gamma}_n$ are both stationary random processes. Also, the pdf of $\hat{\gamma}$ is given by

$$f_{\hat{\gamma}}(\hat{\gamma}) = \frac{\mathrm{U}(\hat{\gamma} - \bar{\gamma}\sigma_{\epsilon_c}^2/\sigma_g^2)}{\bar{\gamma}(1 - \sigma_{\epsilon_c}^2/\sigma_g^2)} \exp\left[-\frac{\hat{\gamma} - \bar{\gamma}\sigma_{\epsilon_c}^2/\sigma_g^2}{\bar{\gamma}(1 - \sigma_{\epsilon_c}^2/\sigma_g^2)}\right], \tag{4}$$

which is a shifted $\chi^2(2)$-distribution, with the shift $\bar{\gamma}\sigma_{\varepsilon_c}^2/\sigma_g^2$ caused by the bias compensation.

III. Average spectral efficiency of adaptive TCM

The spectral efficiency of a (coded) modulation scheme is given by the average data rate per unit bandwidth. Let R_i denote the instantaneous data rate when constellation size M_i is chosen, for $i = 1, \cdots, N$, and W denote the transmitted signal bandwidth. Hence, the average spectral efficiency is simply given by

$$\bar{\eta} = \sum_{i=1}^{N} \frac{R_i}{W} \int_{\hat{\gamma}_i}^{\hat{\gamma}_{i+1}} f_{\hat{\gamma}}(\hat{\gamma}) d\hat{\gamma} \tag{5}$$

where $\{\hat{\gamma}_i\}_{i=1}^{N+1}$, with $\hat{\gamma}_{N+1} = \infty$, denote the rate region boundaries. These thresholds are defined as the ranges of the instantaneous predicted SNR over which different constellations are used by the transmitter, i.e. if $\hat{\gamma} \in [\hat{\gamma}_i, \hat{\gamma}_{i+1})$, k_i coded bits per symbol are transmitted. In other words, a signal constellation or equivalently a transmission rate is assigned to each rate region boundary.

The task here is to find the optimum rate region boundaries such that the average spectral efficiency is maximized subject to two constraints. The first constraint considered in this study is the BER constraint given by

$$\mathrm{BER}_i(\hat{\gamma}) \leq \mathrm{TBER}, \quad \hat{\gamma} \in [\hat{\gamma}_i, \hat{\gamma}_{i+1}), \quad i = 1, \cdots, N, \tag{6}$$

where $\mathrm{BER}_i(\hat{\gamma})$ is the instantaneous BER of the modulation with constellation size of M_i in terms of the instantaneous predicted SNR, and TBER denotes the target BER. This constraint guarantees that the average BER does not exceed the target BER. The second constraint is the use of constant average transmit power. Power adaptation is not included, since the gain achieved in spectral efficiency by rate adaptation is higher than by using power adaptation (at least for adaptive M-QAM) [3] and it increases the complexity.

To find the optimal rate region boundaries based on (6), an expression for $\mathrm{BER}_i(\hat{\gamma})$ is needed. This expression is obtained by averaging $\mathrm{BER}_i(\gamma)$, the instantaneous BER as a function

TABLE I

PARAMETERS $\{a_i(q)\}_{q=1}^3$ AND $\{b_i(q)\}_{q=1}^3$ OF TCM CODES.

i	$a_i(1)$	$b_i(1)$	$a_i(2)$	$b_i(2)$	$a_i(3)$	$b_i(3)$
1	30.9487	11.4545	-105.9332	9.8150	75.5856	9.1826
2	15.4067	6.7158	-77.7363	5.8901	62.6452	5.6452
3	91.3050	8.4824	-194.7515	7.7474	104.3384	7.1502
4	89.9720	8.2248	-168.6707	8.9040	72.3208	9.6999
5	120.4751	8.1244	-184.9618	8.5936	65.0278	9.4727
6	303.5932	8.6210	-375.4897	8.8549	74.4199	9.8427
7	192.5175	8.3420	-295.9806	8.7070	103.9613	9.3817

of the instantaneous true SNR, γ, on an AWGN channel, over all values of γ, i.e.

$$\mathrm{BER}_i(\hat{\gamma}) = \int_0^\infty \mathrm{BER}_i(\gamma) f_\gamma(\gamma|\hat{\gamma}) d\gamma, \; i = 1, \cdots, N, \quad (7)$$

where $f_\gamma(\gamma|\hat{\gamma})$ is given by (3). Hence, what remains is to determine $\mathrm{BER}_i(\gamma)$ which will be discussed next.

Tight approximations for the TCM BER performance on AWGN channels at high SNR, based on analytical or numerical methods, are available in the literature [7]. However, to perform the integration in (7), an expression which approximates the BER well enough over the *whole range* of SNRs is required. This expression is preferred to be in a form that results in a closed form expression for $\mathrm{BER}_i(\hat{\gamma})$ based on (7). This simplifies the search for optimal thresholds. In this study, considering the formulation of $f_\gamma(\gamma|\hat{\gamma})$ given by (3), a general expression given by [12]

$$\mathrm{BER}_i(\gamma) \approx \sum_{q=1}^{Q} a_i(q) \exp\left[-b_i(q)\gamma\right], \quad i = 1, \cdots, N, \quad (8)$$

assures fulfilling the above mentioned requirements. Here, the parameters $\{a_i(q)\}_{q=1}^Q$ and $\{b_i(q)\}_{q=1}^Q$, are real numbers where the latter set takes only non-negative values. Both sets are determined by using curve fitting with least squares techniques utilizing the simulated BER for different constellation sizes on AWGN channels. Examples are shown in Section IV. Consequently, using (3) and (8) in (7), leads to

$$\mathrm{BER}_i(\hat{\gamma}) \approx \sum_{q=1}^{Q} \frac{a_i(q)}{1 + b_i(q)\bar{\gamma}\frac{\sigma_{\epsilon_c}^2}{\sigma_g^2}} \exp\left[-\frac{b_i(q)(\hat{\gamma} - \bar{\gamma}\frac{\sigma_{\epsilon_c}^2}{\sigma_g^2})}{1 + b_i(q)\bar{\gamma}\frac{\sigma_{\epsilon_c}^2}{\sigma_g^2}}\right], \quad i = 1, \cdots, N. \quad (9)$$

The optimal rate region boundaries, $\{\hat{\gamma}_i\}_{i=1}^N$, are found by solving (6) with equality where (9) is used to approximate $\mathrm{BER}_i(\hat{\gamma})$. An analytical expression for the optimal rate region boundaries can be found for $Q = 1$. If $Q > 1$, numerical approaches such as the *bisection method* [13] can be used to find the optimal thresholds. Once they are evaluated, the spectral efficiency can easily be obtained according to (5).

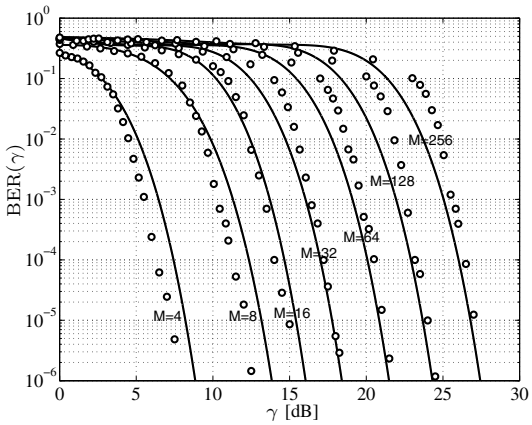

Fig. 1. BER performance of TCM codes on AWGN channels where M denotes the constellation size. The curves are approximations obtained from (8) and the circles are outcomes of simulation.

IV. RESULTS AND DISCUSSION

The illustrative example considered here is given for the 4-D TCM (i.e. $L = 2$) with 16 states, utilizing a rate $2/3$ convolutional encoder and a bit mapper similar to those used in the International Telecommunication Union's ITU-T V.34 modem standard. Nyquist pulse shaping, i.e. $W = 1/T_s$, and $N = 7$ 2-D signal constellations of sizes $M_i \in \{4, 8, 16, 32, 64, 128, 256\}$, corresponding to 4-QAM, 8-STAR, 16-QAM, 32-CROSS, 64-QAM, 128-CROSS and 256-QAM, respectively, are presumed. At each even time instant, $2 \times k_i - 1$ information bits are encoded to $2 \times k_i$ coded bits which are mapped onto two symbols, each from a 2-D constellation of size M_i. These symbols are transmitted during the next two time instants and result in a instantaneous data rate given by $R_i = (k_i - 1/2)W$.

The BER performance of the above mentioned trellis-codes on AWGN channels was simulated for various SNRs. As explained in Section III, the simulation outcomes were used to approximate the BER for AWGN channels based on (8). The resulting parameters are listed in Table I. The BER approximations are depicted in Fig. 1 and compared with the simulated BERs for different constellation sizes. It is clear that the approximations are tight within 1.5 dB in comparison with the simulated results.

Based on these approximations, the performance of the adaptive TCM scheme for flat Rayleigh fading channels with average power $\sigma_g^2 = 1$, is evaluated. The results are compared to those of the uncoded adaptive M-QAM scheme [4] utilizing the same signal constellations as the adaptive TCM but having the instantaneous data rate given by $R_i = k_i W$.

Fig. 2 shows the average spectral efficiency, $\bar{\eta}$, versus the average SNR, $\bar{\gamma}$, for $\mathrm{TBER} = 10^{-3}$ and 10^{-5}, and prediction error variances $\sigma_{\epsilon_p}^2 = 0.01$ and 0.1. The results demonstrate that in a large range of average SNR, the adaptive TCM somewhat outperforms the adaptive uncoded M-QAM (by 1-2 dB). The spectral efficiency curves flatten out due to the limited number of data rates.

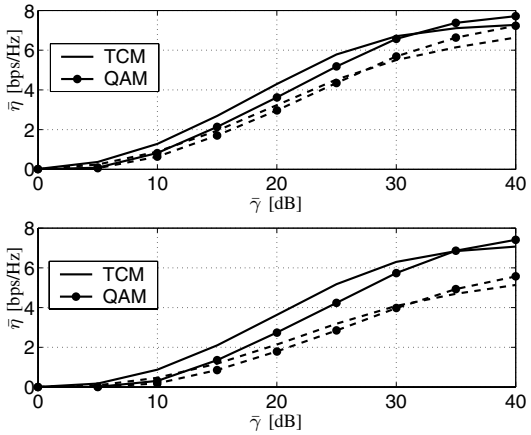

Fig. 2. The average spectral efficiency of the adaptive transmission based on TCM and uncoded M-QAM schemes versus average received SNR. The upper and lower plots correspond to $\mathrm{TBER} = 10^{-3}$ and 10^{-5}, respectively. The solid and dashed lines correspond to $\sigma^2_{\epsilon_p} = 0.01$ and 0.1, respectively.

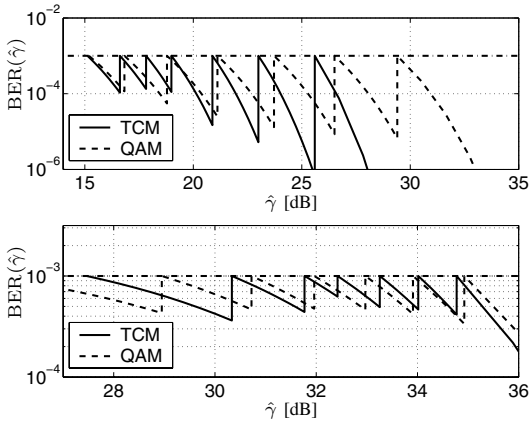

Fig. 3. Instantaneous BER versus instantaneous predicted SNR of the adaptive transmission based on TCM and uncoded M-QAM schemes for $\mathrm{TBER} = 10^{-3}$ and $\sigma^2_{\epsilon_p} = 0.1$. The upper and lower plots correspond to $\bar{\gamma} = 20$ dB and 40 dB, respectively.

An interesting phenomenon observed here is that the gain by TCM gradually vanishes as the average SNR increases. This effect is more pronounced for small TBERs and large prediction error variances. At high average SNRs, the transmitter often transmits at the highest data rate which happens to be larger for uncoded M-QAM than TCM, and hence, provides a higher spectral efficeincy. In addition, there is a non-intuitive effect due to the influence of the prediction quality on the location of the rate region boundaries. Fig. 3 displays *how* the SNR thresholds for $\mathrm{TBER} = 10^{-3}$ vary as $\bar{\gamma}$ increases. At $\bar{\gamma} = 20$ dB, the adaptive TCM has lower thresholds as compared to uncoded M-QAM and achieves a higher average spectral efficiency as shown in Fig. 2. However, at $\bar{\gamma} = 40$ dB, the uncoded M-QAM exhibits *lower* thresholds for smaller constellations and higher spectral efficiency. To explain *why* the rate region boundaries behave in this way, the integrands and outcome of the integral in (7) are illustrated graphically in Fig. 4.

On AWGN channels for a given SNR, as shown in Fig. 4-(a), lower BER is obtained by TCM as compared to uncoded QAM, *except* for a limited range of low SNRs (this is typical for coded modulations). After performing the integration in (7), this feature is preserved for the predicted BER. Comparing Fig. 4-(a) and 4-(c) shows: TCM begins to outperform uncoded QAM at a *lower* BER as compared to the case for AWGN channels. It is observed (but not shown here) that the predicted SNR value corresponding to the starting point of better performance of TCM than uncoded M-QAM, increases as the tail of the pdf $f_\gamma(\gamma|\hat{\gamma})$ in (3) becomes heavier. This tail is strongly influenced by the ratio between the predicted and average SNRs. In a fading dip, i.e. when $\gamma < \bar{\gamma}$, the predictor basically fails in making a good prediction and results in a large prediction error variance *relative* to the predicted SNR. When the temporary channel condition improves , i.e. when $\gamma > \bar{\gamma}$, the channel prediction accordingly becomes more accurate. This yields a smaller error variance relative to the predicted value.

Fig. 4-(b) shows how the shape of $f_\gamma(\gamma|\hat{\gamma})$ varies for different values of the average SNR, given $\hat{\gamma}$ and $\sigma^2_{\epsilon_p}$ are constant. At $\bar{\gamma} = 20$ dB, the pdf which is centered around $\gamma = 30$ dB and has small tails, shows the channel quality is above the average and the prediction of $\hat{\gamma} = 30$ dB is close to the actual value. For $\bar{\gamma} = 30$ dB, the conditional pdf becomes more spread around $\gamma = 30$ dB with heavier tails, meaning that the prediction of $\hat{\gamma} = 30$ dB contributes in more errors. Finally, at $\bar{\gamma} = 40$ dB where the predicted SNR is far below the average, the tail of the pdf below $\gamma = 30$ dB, grows substantially. This indicates that the predicted value is unreliable and the channel experiences a fading dip. More examples of this property are given in Fig. 5, which shows how the average SNR affects some of the rate boundaries of adaptive uncoded M-QAM and TCM accordingly, for the given $\mathrm{TBER} = 10^{-3}$ and $\sigma^2_{\epsilon_p} = 0.1$.

Finally Fig. 6 illustrates how the prediction quality influences the data rate of the adaptive scheme. The spectral efficiency decreases as the predictor degrades, as demonstrated in Fig. 2. This stems from the fact that the rate boundaries are increased as the prediction error variance increases as displayed in Fig. 6, where the average SNR and TBER remain constant. Also, a larger variation in thresholds for smaller constellations is observed here. This is simply because higher data rates are used for channels that are predicted to be in favorable conditions. In those cases, the prediction errors can hardly change the channel status and impose a lower data rate.

Note that since the above conclusions are drawn based on the *relative* BER performance of TCM and uncoded M-QAM, they remain valid also for better approximations (compare the simulation results in Fig. 1 here with the BER performance in Fig. 2 of [3]).

V. Conclusions

The optimum design of an adaptive scheme based on TCM that utilizes imperfectly predicted CSI for flat Rayleigh fading

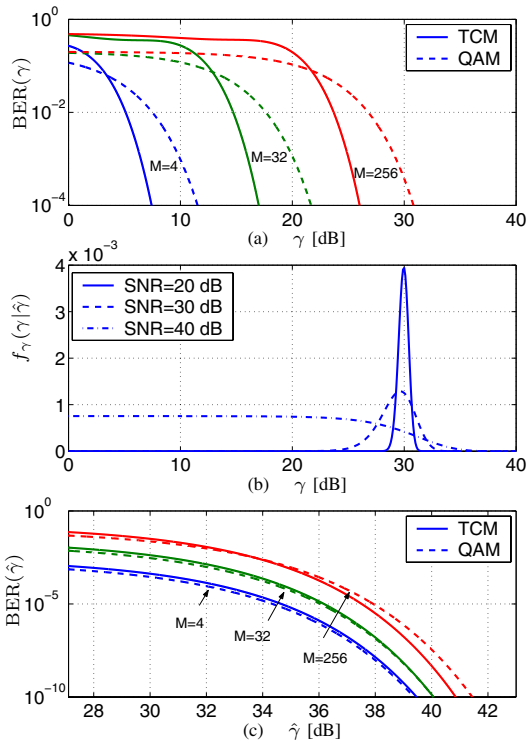

Fig. 4. Plot (a) illustrates the instantaneous BER on AWGN channels versus instantaneous SNR. Plot (b) shows the conditional pdf given by (3), for $\hat{\gamma} = 30$ dB and $\sigma^2_{\epsilon_p} = 0.1$. Plot (c) displays the instantaneous BER versus instantaneous predicted SNR for $\bar{\gamma} = 40$ dB and $\sigma^2_{\epsilon_p} = 0.1$.

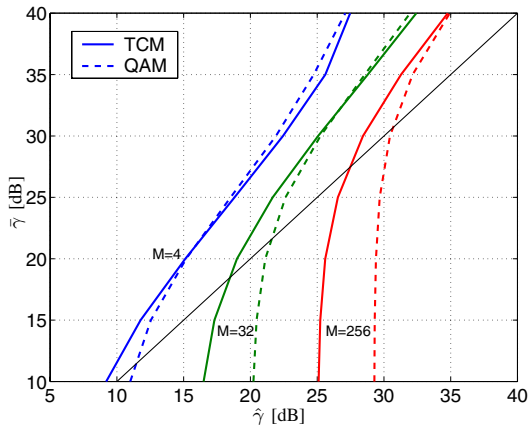

Fig. 5. Optimum rate region boundaries in terms of the average SNR for $\mathrm{TBER} = 10^{-3}$ and $\sigma^2_{\epsilon_p} = 0.1$. The diagonal line corresponds to $\hat{\gamma} = \bar{\gamma}$.

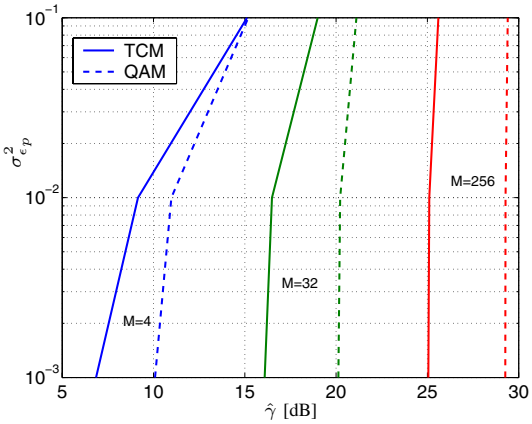

Fig. 6. Optimum rate region boundaries in terms of the prediction error variance for $\mathrm{TBER} = 10^{-3}$ and $\bar{\gamma} = 20$ dB.

channels, is investigated. Assuming constant average transmit power, the data rate is adjusted based on the predicted SNR and the prediction error variance to maximize the spectral efficiency and satisfy a BER requirement. The adaptive TCM is compared to an adaptive uncoded M-QAM scheme from the performance point of view. The results indicate that the former increases the spectral efficiency for a large but limited range of average SNR as compared to the latter. At high average SNR, uncoded M-QAM outperforms TCM due to the higher data rate or (and) the lower thresholds for smaller constellations. The impact is more pronounced for small TBERs and large prediction error variances. The SNR thresholds above the average SNR are not affected much by prediction errors, while those below the average are raised considerably. This effect increases with the prediction error variance.

REFERENCES

[1] A. J. Goldsmith and S. Chua, "Variable-rate variable-power MQAM for fading channels," *IEEE Transactions on Communications*, vol. 45, no. 10, pp. 1218–1230, Oct. 1997.

[2] M.-S. Alouini and A. J. Goldsmith, "Adaptive M-QAM modulation over Nakagami fading channels," *Kluwer Wireless Personal Comm.*, vol. 13, pp. 119–143, May 2000.

[3] S. T. Chung and A. J. Goldsmith, "Degrees of freedom in adaptive modulation: a unified view," *IEEE Transactions on Communications*, vol. 49, no. 9, pp. 1561–1571, Sept. 2001.

[4] S. Falahati, A. Svensson, M. Sternad, and T. Ekman, "Adaptive modulation systems for predicted wireless channels," in *Proc. IEEE Global Telecommunications Conference*, San Francisco, USA, Dec. 2003.

[5] S. M. Alamouti and S. Kallel, "Adaptive trellis-coded multiple-phase-shift keying for Rayleigh fading channels," *IEEE Transactions on Communications*, vol. 42, no. 6, pp. 2305–2314, June 1994.

[6] A. J. Goldsmith and S. Chua, "Adaptive coded modulation for fading channels," *IEEE Transactions on Communications*, vol. 46, no. 5, pp. 595–602, May 1998.

[7] K. J. Hole, H. Holm, and G. E. Øien, "Adaptive multidimensional coded modulation over flat fading channels," *IEEE Journal on Selected Areas in Communications*, vol. 18, no. 7, pp. 1153–1158, July 2000.

[8] V. K. N. Lau and M. D. Macleod, "Variable-rate trellis coded QAM for flat-fading channels," *IEEE Transactions on Communications*, vol. 49, no. 9, pp. 1550–1560, Sept. 2001.

[9] D. L. Goeckel, "Adaptive coding for time-varying channels using outdated fading estimates," *IEEE Transactions on Communications*, vol. 47, no. 6, pp. 844–855, June 1999.

[10] T. Ekman, M. Sternad, and A. Ahlén, "Unbiased power prediction on broadband channel," in *Proc. IEEE Vehicular Technology Conference*, Vancouver, Canada, Sept. 2002.

[11] T. Ekman, "Prediction of mobile radio channels, modeling and design," PhD thesis, Signals and Systems, Uppsala University, Uppsala, Sweden. http://www.signal.uu.se/Publications/abstracts/a023.html, Oct. 2002.

[12] I. S. Gradshteyn and I. M. Ryzhik, *Table of Integrals, Series and Products*, Academic Press, San Diego, CA, 5th edition, 1994.

[13] W. H. Press, S. A. Teukolsky, W. T. Vetterling, and B. P. Flannery, *Numerical Recipes in C*, Cambridge, U.K., 2nd edition, 1997.